**Chapman University**
## Chapman University Digital Commons

Mathematics, Physics, and Computer Science
Faculty Articles and Research

Science and Technology Faculty Articles and Research

1993

# Extended Variability of the Symbiotic Star AG Draconis

Menas Kafatos
*Chapman University*, kafatos@chapman.edu

S. R. Meier
*USN, Res Lab*

Follow this and additional works at: http://digitalcommons.chapman.edu/scs_articles

Part of the Instrumentation Commons, and the Stars, Interstellar Medium and the Galaxy Commons

### Recommended Citation

# Extended Variability of the Symbiotic Star AG Draconis

**Comments**

**Copyright**

# EXTENDED VARIABILITY OF THE SYMBIOTIC STAR AG DRACONIS

M. KAFATOS AND S. R. MEIER[1]
Department of Physics and CSI Institute, George Mason University, Fairfax, Virginia 22030-4444
AND
I. MARTIN[2]
CSI Institute, George Mason University
*Received 1991 November 15; accepted 1992 July 24*

## ABSTRACT

We have analyzed the complete set of available *IUE* (*International Ultraviolet Explorer*) spectra for the symbiotic star AG Draconis covering the period from 1979 to 1989. All absolute line fluxes and wavelengths have been obtained for the prominent emission lines in the $\lambda\lambda 1200$–3200 wavelength range. These spectra contain observations which were taken before, during and after the two extended outbursts which occurred on 1980 November to 1981 November and 1985 February to 1986 January. These two outburst events have two maxima that are separated by $\sim 1600$ days, a time scale not known to be associated with the star, but which is $\sim 3$ times the binary period of the star. O IV] $\lambda\lambda 1397$–1407 emission line intensities imply an electron density in the range $10^{10} \leq n_e \leq 10^{11}$ cm$^{-3}$. We found the line-emitting region to have a linear size $10^{12} \leq L \leq 10^{13}$ cm. The He II $\lambda 1640$ Zanstra method yields $T_* \geq 87,000$ K for the hot component.

Absolute line intensities are plotted as a function of Julian Date for the principal emission lines of N V $\lambda\lambda 1238$, 1242, O I $\lambda\lambda 1302$–1306, O IV] $\lambda\lambda 1397$–1407, C IV $\lambda\lambda$ 1548, 1550, He II $\lambda 1640$ and O III] $\lambda\lambda 1660$, 1666 to observe the temporal variability of AG Dra. Emission line fluxes of N V, O I, N IV], C IV, and N III] are plotted as a function of C IV to study the nature of the emitting regions. We have calculated the nitrogen ionic abundances for AG Dra to study how the ionization levels change during outburst and quiescence phases of the star. The time-evolution of the calculated ionic abundances shows the presence of abundance peaks coincident with the outburst events and the binary phases favoring episodic mass transfers onto the compact star. Monitoring, preferably every 3 to 4 years could be helpful in confirming the accretion-powered outburst mechanism of this star and provide important insights into the symbiotic phenomenon in general.

*Subject headings:* binaries: symbiotic — stars: individual (AG Draconis) — ultraviolet: stars

## 1. INTRODUCTION

The symbiotic star AG Draconis (BD + 67°922) was first discovered by Janssen & Vyssofsky (1943). When the first high-dispersion optical spectra were taken by Wilson (1943), AG Dra displayed strong emission lines of H I and He II. AG Draconis has been classified as a high-velocity (Roman 1953), high Galactic latitude star ($l = 100°$, $b = +41°$). The binary system of AG Draconis consists of a hot star and a cool K giant of a controversial spectral class. Kenyon & Webbink (1984) consider it to be of K3 III type, whereas Lutz et al. (1987) assign a luminosity class III and K1 type to the primary, and Allen (see Kenyon 1986) assumes it to be of K1 ± 1 III type. Finally, Kenyon & Fernandez-Castro (1987) found the cool star to be earlier than K4 III from infrared data. Friedjung (1988) claims the luminosity of the cool star to be uncertain, preventing a correct model for the binary to be proposed. A photometric period of 554 days and corresponding ephemeris of Max (U) = JD 2438900 + 554E has been determined by Meinunger (1979), and confirmed by Oliversen & Anderson (1982) using a larger data set. The radial velocity of the absorption line system is $\sim 140$ km s$^{-1}$ (Roman 1953; Huang 1982).

A strong X-ray flux was detected with the *Einstein HEA0 2* satellite that corresponds to a $T < 2 \times 10^6$ K thermal emitting source (Anderson et al. 1981). An interesting feature is the anticorrelation between the X-ray flux and the last UV maximum of 1986 February (Cassatella et al. 1987). The observations obtained with *EXOSAT* (Friedjung 1988) show no X-ray detection in 1986 February, following a new increase in overall luminosity. The *EXOSAT* observations are also discussed by Viotti (1993).

*IUE* spectra taken of AG Dra are characterized by a strong continuum with intense permitted (e.g. N V $\lambda\lambda 1238$, 1242, C IV $\lambda\lambda 1548$, 1550, He II $\lambda 1640$) and weak intersystem emission lines (e.g. O IV] $\lambda\lambda 1397$–1407, N III] $\lambda\lambda 1747$–1753, Si III] $\lambda 1892$, C III] $\lambda\lambda 1907$, 1909) (Lutz & Lutz 1981; Altamore et al. 1982; Viotti et al. 1982, 1983, 1984; Lutz et al. 1987). During an active phase, emission line intensities are generally stronger by factors of $\sim 3$–10 as compared to quiescent line intensities and the UV continuum can be as high as 10 times the quiescence level (Mürset et al. 1991).

It is not clear if the interstellar extinction varies between quiescence and active phases, therefore, Kenyon (1986) gives two fittings that range $E_{B-V} = 0.01$ and 0.04, while Viotti et al. 1983 found $E_{B-V} = 0.06 \pm 0.03$. Using the extinction curves of

[1] Postal address: University of Southern California, Department of Physics and Astronomy, Los Angeles, CA 90089.
[2] Postal address: Departamento De Quimica Fisica, Facultad De Ciencias, Universidad De Valladolid, 47005 Valladolid, Spain.

KAFATOS, MEIER, & MARTIN

Seaton (1978, 1979) and the theoretical ratios of the He II $\lambda3203/\lambda1640$ lines (Osterbrock 1989), we determined $E_{B-V}$ $\sim 0.03$ for both quiescent and active phases. This value is within the uncertainty of the Viotti et al. (1983) value. Therefore, we adopt a value of $E_{B-V} = 0.06$.

Several outbursts followed by long periods of quiescence have long been recognized for this star (Robinson 1969). Kaler et al. (1987), using optical photometry and AAVSO data, found two maxima associated with each of the two outbursts (1980–1981 and 1985–1986). The 1980–1981 outburst had two maxima at $\sim 2444600$ and $2445000$, while the 1985–1986 outburst had two similar maxima at $\sim 2446100$ and $2446500$. Recently, Iijima (1987) using photometric light curves taken since 1930, proposed that AG Dra becomes active every 15 years. He derived an activity cycle or ephemeris of JD (active) = $2422660 + 5540E$ (days), which corresponds to 10 cycles of the 554 day period. However, Cassatella et al. (1987) found the star in an outburst phase in 1985 February and 1986 January. This UV outburst with two maxima anomalously occurred 4 and 5 years after the 1980/1981 outbursts, which is approximately three cycles of the 554 day binary period.

In this paper, we present the high- and low-resolution $IUE$ satellite observations of AG Draconis covering the period 1979–1989. This work presents a comprehensive study of all the far-UV spectra taken of AG Dra. We are primarily concerned with the analysis and interpretation of these ultraviolet observations and what they imply for the nature of the system. In § 2, line intensities of the high- and low-dispersion spectra of AG Dra are presented along with representative figures of the UV line fluxes. Our calculations of $n_e$, $L$, photoionization parameters, etc., are discussed in the § 3. Finally, in § 4 we give our interpretations and conclusions.

## 2. ULTRAVIOLET OBSERVATIONS

Approximately, 29 low-resolution (LORES) SWP, 14 LWR, and 13 LWP and eight high-resolution (HIRES) SWP, LWP, and LWR $IUE$ spectra have been reduced and calibrated. These spectra cover three quiescent and two outburst

phases of AG Dra between 1979 and 1989. All absolute line fluxes and wavelengths have been obtained for the prominent emission lines in the $\lambda\lambda1200$–3200 wavelength range. The ultraviolet spectra analyzed were obtained with the large aperture ($10'' \times 20''$) $IUE$ spectrometer, which has a limiting spectral resolution in low dispersion of $\sim 6$ Å and $\sim 0.1$ Å for high dispersion spectra, respectively. The $IUE$ data shown were reduced and analyzed with the data reduction routines in IDL (interactive design language) developed at the RDAF (Reduction Data Analysis Facility) at NASA/GSFC. All LWP/LWR spectra have been reprocessed using the most recent ITF (intensity transfer function). Moreover, all high-dispersion and low-dispersion spectra have been corrected for interstellar extinction using the Savage & Mathis (1979) method with an $E_{B-V} = 0.06$ (Viotti et al. 1983).

In Table 1, we have recorded the observational parameters for all low resolution and high resolution SWP, LWP and LWR spectra shown in the figures. These spectra represent a partial list of the images analyzed. We have chosen $IUE$ spectra that best represent the many quiescent and active periods of AG Dra.

Tables 2A and 2B give the dereddened absolute line intensities for the most prominent emission lines in the LORES mode for the SWP ($\lambda\lambda1200$–2000) and LWP/LWR ($\lambda\lambda2000$–3200) wavelength ranges. As can be seen from Table 2A, highly excited ions such as N V $\lambda\lambda1238$, 1242, N IV] $\lambda1487$, C IV $\lambda\lambda1548$, 1550 and He II $\lambda1640$ have active fluxes which are $\sim 5$ times the quiescent values. However, many of the He II fluxes, particularly during outburst, were overexposed. He II $\lambda1640$ is the dominant UV line for both quiescent and active phases, a highly unusual case for symbiotic stars in general. Most of the semi-forbidden emission lines longward of $\lambda1700$Å (e.g. N III] $\lambda\lambda1747$–1753, Si III] $\lambda1892$, C III] $\lambda\lambda1907$, 1909) are very weak or not even present in either quiescence or outburst phases. Finally, in the LWP/LWR wavelength region, line intensities differ by as much as factor of $\sim 10$ or larger between outburst and quiescent states for O III $\lambda\lambda3122$, 3133 and He II $\lambda3203$. However, the uncertainty in these emission lines is large because they are near the end of the LWP detector.

Figures 1a–1h show LORES SWP and LWP/LWR spectra

### TABLE 1
### LIST OF $IUE$ OBSERVATIONS

| Camera/Image Sequence Number | Julian Date | Date | Dispersion | Start (UT) | Exposure (minutes) | State of System |
|---|---|---|---|---|---|---|
| LWR 11231 ...... | 2444820 | 1981 Aug 3 | Low | 22 32 | 05 | Active |
| SWP 14640 ...... | 2444820 | 1981 Aug 3 | Low | 20 33 | 15 | Active |
| LWR 12124 ...... | 2444950 | 1981 Dec 11 | High | 10 34 | 40 | Active |
| SWP 15710 ...... | 2444950 | 1981 Dec 11 | High | 11 22 | 120 | Active |
| SWP 20162 ...... | 2445493 | 1983 June 7 | High | 02 36 | 140 | Quiescent |
| LWP 3920 ....... | 2445916 | 1984 Aug 3 | Low | 22 12 | 15 | Quiescent |
| SWP 23582 ...... | 2445916 | 1984 Aug 3 | Low | 21 01 | 20 | Quiescent |
| LWP 5514 ....... | 2446138 | 1985 Mar 13 | High | 09 44 | 33 | Active |
| SWP 25544 ...... | 2446138 | 1985 Mar 13 | High | 08 49 | 50 | Active |
| LWP 7522 ....... | 2446449 | 1986 Jan 18 | Low | 03 57 | 06 | Active |
| SWP 27542 ...... | 2446449 | 1986 Jan 18 | Low | 04 18 | 10 | Active |
| SWP 37473 ...... | 2447827 | 1989 Oct 27 | Low | 16 37 | 25 | Quiescent |
| LWP 16674 ...... | 2447827 | 1989 Oct 27 | High | 15 37 | 30 | Quiescent |
| SWP 37475 ...... | 2447828 | 1989 Oct 28 | High | 14 12 | 60 | Quiescent |
| LWP 16683 ...... | 2447828 | 1989 Oct 28 | Low | 15 21 | 10 | Quiescent |

TABLE 2A
LOW-RESOLUTION SWP λλ1200–2000 SPECTRA OF AG DRACONIS

| Ion | λ(Lab) (Å) | λ(IUE) (Å) | ABSOLUTE FLUX (10⁻¹² ergs cm⁻² s⁻¹) | | | |
|---|---|---|---|---|---|---|
| | | | 14640 Active | 23582 Quiescent | 27542 Active | 37473 Quiescent |
| N v ......... | 1238.8, 1242.8 | 1238.9 | 56.0[a] | 7.8 | 49.9[a] | 9.4 |
| Si ii ......... | 1264.9 | 1263.2 | 2.9 | 0.4 | | 0.3 |
| O i .......... | 1301.1, 1304.9, 1306.01 | 1303.8 | | | 2.1 | 1.0 |
| C ii ......... | 1334.5, 1335.7 | | | | | |
| Si iv ........ | 1393.8 | 1393.0 | 6.7[a] | 1.7 | 9.0 | 1.5 |
| O iv] ........ | 1397.2, 1399.8, 1401.1, 1404.8, 1407.3 | 1401.0 | 21.8[a] | 4.6 | 32.3 | 4.5 |
| N iv] ........ | 1483.3, 1486.5 | 1485.5 | 7.5 | 1.6 | 8.8 | 1.8 |
| C iv ......... | 1548.2, 1550.8 | 1548.3 | 41.0[a] | 6.5 | 53.9[a] | 7.9 |
| [Ne v] ....... | 1574.7 | 1576.1 | 1.4 | | 1.0[b] | 0.2 |
| [Ne iv] ...... | 1601.5 | 1601.7 | | 0.2[b] | | |
| He ii ........ | 1640.4 | 1639.3 | 57.9[a,c] | 22.5[a] | 110.0[a,c] | 22.9[a] |
| O iii] ........ | 1660.8, 1666.1 | 1664.0 | 6.5 | 1.8 | 5.1 | 2.5 |
| N iv ........ | 1718.5 | 1718.4 | 0.6[b] | 0.5 | 0.8 | 0.4 |
| N iii] ........ | 1746.8, 1748.6, 1749.6, 1752.1, 1753.9 | 1748.8 | 0.4[b] | 0.3 | | 0.7 |
| Si ii ......... | 1808.0, 1816.9, 1817.4 | 1817.9 | 0.6 | | 1.1 | |
| Si iii] ........ | 1892.0 | 1891.2 | 2.2 | 0.5 | 2.0 | 0.4[b] |
| C iii] ........ | 1906.7, 1908.7 | 1910.5 | | | 0.4[b] | 0.1[b] |

[a] Saturated.
[b] Weak feature.
[c] Broad feature.

in active and quiescent states of the star. These spectra were selected because they have the best signal-to-noise ratio and are representative of the star in activity and quiescence. Figures 1a and 1e (SWP 14640, LWR 11231) show the star in an outburst state in 1981 August. The Figures 1b and 1f (SWP 23582, LWP 3920) represents the quiescent state of AG Dra, these spectra were taken in 1984 August. The next outburst which took place in 1986 January is shown in Figures 1c and 1g (SWP 27542, LWP 7522). Finally, Figures 1d and 1h (SWP

37473, LWP 16683) show the star in a quiescent phase in 1989 October.

Tables 3A and 3B give the line intensities and corresponding wavelengths for all the HIRES SWP, LWP, and LWR spectra. The emission line fluxes in the HIRES SWP wavelength region vary only by factors of ∼3–5 between active and quiescent states. Figures 2a–2b, 3a–3b, 4a–4b, 5a–5b, and 6a–6b show HIRES spectra of highly excited individual ions (N v, C iv), medium excitation ions (Si iv + O iv], O iii]), and low excita-

TABLE 2B
LOW-RESOLUTION LWP/LWR λλ2000–3200 SPECTRA OF AG DRACONIS

| Ion | λ(Lab) (Å) | λ(IUE) (Å) | ABSOLUTE FLUX (10⁻¹² ergs cm⁻² s⁻¹) | | | |
|---|---|---|---|---|---|---|
| | | | 11231 Active | 3920 Quiescent | 7522 Active | 16683 Quiescent |
| He ii ...... | 2252.7 | 2250.2 | 5.8 | | 2.8 | 0.2[a] |
| C ii] ...... | 2326.9, 2328.1 | 2327.7 | 1.4 | 0.4[a] | 0.9 | 0.2[a] |
| [O ii] ...... | 2470.3 | 2470.4 | | 0.6[a] | | 0.1[a] |
| He ii ...... | 2511.2 | 2508.0 | 5.0 | 1.1 | 6.7[b] | 0.7 |
| He ii ...... | 2733.3 | 2728.0 | 11.5[b] | 1.1 | 3.9[b] | 0.9 |
| Mg ii ...... | 2795.4, 2797.9, 2802.6 | 2794.2 | 13.9[b] | 1.9 | 2.1[b] | 2.5 |
| O iii ...... | 2818.7 | 2816.0 | 3.2 | | | 0.1[a] |
| O iii ...... | 2826.6 | 2833.2 | 4.0 | 0.2[a] | | 0.2 |
| O iii ...... | 3121.6 | 3116.7 | 4.4 | 0.3[a] | 5.2[b] | 0.2 |
| O iii ...... | 3132.9 | 3128.1 | 5.9 | 0.9 | 10.4[b] | 0.9 |
| He ii ...... | 3203.0 | 3197.0 | 6.9 | 2.8 | 16.5 | 1.8 |

[a] Saturated.
[b] Weak feature.
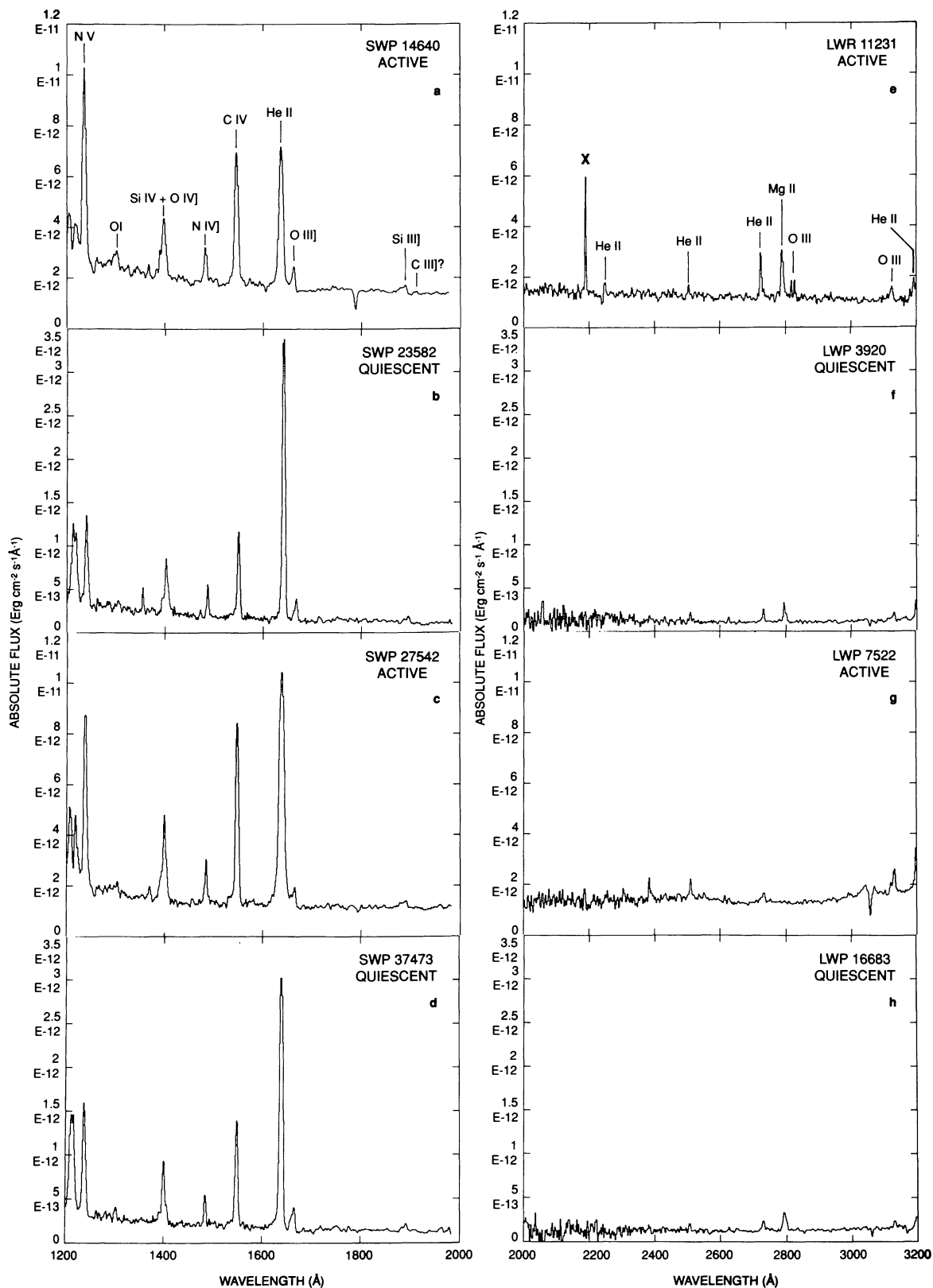
FIG. 1.—Low-resolution *IUE* spectra of AG Draconis obtained in the SWP λλ1200–2000 and LWP/LWR λλ2000–3200 wavelength regions for four observing dates (1981 August, 1984 August, 1986 January, 1989 October). These spectra represent two of the active and quiescent phases of AG Draconis. Note the variations in the UV continuum between activity and quiescence. All spectra have been corrected for interstellar extinction $E_{B-V} = 0.06$. Units are in ergs cm$^{-2}$ s$^{-1}$ Å$^{-1}$. "$X$" indicates a cosmic ray hit.

TABLE 3A

HIGH-RESOLUTION SWP λλ1200–2000 SPECTRA OF AG DRACONIS

| Ion | SWP 15710 ACTIVE | | SWP 20162 QUIESCENT | | SWP 25444 ACTIVE | | SWP 37475 QUIESCENT | |
|---|---|---|---|---|---|---|---|---|
| | λ(IUE) (Å) | Absolute Flux[a] | λ(IUE) (Å) | Absolute Flux[a] | λ(IUE) (Å) | Absolute Flux[a] | λ(IUE) (Å) | Absolute Flux[a] |
| N v ....... | 1238.21 | 32.2 | 1238.22 | 16.2 | 1238.21 | 30.2 | 1238.22 | 6.3 |
| N v ....... | 1242.38 | 18.8 | 1242.28 | 6.0 | 1242.29 | 9.3 | 1242.27 | 1.6 |
| O i ........ | 1301.52 | 2.1 | 1301.53 | 0.8 | ... | ... | ... | ... |
| Si iv ....... | 1393.04 | 4.9 | 1393.09 | 1.7 | 1393.11 | 2.9 | 1393.08 | 0.4 |
| O iv] ...... | 1399.01 | 1.4 | 1399.05 | 1.2 | 1399.04 | 1.7 | 1399.00 | 0.8 |
| O iv] ...... | 1400.39 | 6.2 | 1400.47 | 4.5 | 1400.42 | 8.3 | 1400.45 | 1.7 |
| O iv] ...... | 1402.07 | 3.9 | 1402.09 | 1.0 | 1402.07 | 1.3 | ... | ... |
| O iv] ...... | 1404.06 | 2.1 | 1404.11 | 1.6 | 1404.09 | 2.3 | 1404.13 | 0.5 |
| O iv] ...... | 1406.64 | 1.3 | 1406.67 | 0.7 | 1406.65 | 1.4 | 1406.66 | 0.6 |
| N iv] ...... | 1485.75 | 6.0 | 1485.78 | 2.7 | 1485.75 | 4.0 | 1485.74 | 1.4 |
| C iv ....... | 1547.41 | 36.0 | 1547.46 | 9.0 | 1547.44 | 26.1 | 1547.50 | 4.0 |
| C iv ....... | 1549.98 | 24.0 | 1550.04 | 5.0 | 1550.12 | 14.3 | 1550.05 | 2.4 |
| He ii ...... | 1639.46 | 135.0[b] | 1639.54 | 34.5[b] | 1639.54 | 139.0[b] | 1639.57 | 25.2 |
| O iii] ...... | 1659.92 | 1.0 | 1659.99 | 0.7 | 1659.99 | 1.2 | 1659.95 | 0.7 |
| O iii] ...... | 1665.32 | 3.4 | 1665.32 | 2.0 | 1665.29 | 3.5 | 1665.29 | 0.8 |
| N iii] ...... | 1748.81 | 0.3 | ... | ... | ... | ... | 1748.95 | 1.1 |
| N iii] ...... | ... | ... | 1750.11 | 0.4 | 1750.19 | 0.8 | 1750.33 | 0.3 |
| N iii] ...... | ... | ... | ... | ... | 1751.03 | 0.7 | 1751.43 | 0.2 |
| Si ii ....... | 1810.23 | 0.2 | 1810.07 | 0.1 | 1810.12 | 0.2 | ... | ... |
| Si iii] ...... | 1883.27 | 0.3 | 1883.23 | 0.2 | 1883.16 | 0.3 | 1883.25 | 0.2 |
| Si iii] ...... | 1891.10 | 1.3 | 1891.11 | 1.0 | 1891.09 | 0.6 | 1891.13 | 0.6 |
| C iii ....... | 1907.81 | 0.6 | 1907.83 | 0.3 | 1907.84 | 0.3 | ... | ... |

[a] Fluxes are in units of $10^{-12}$ ergs cm$^{-2}$ s$^{-1}$.
[b] Saturated.

tion states (Mg ii) in the outburst and quiescent phases of the star. As before, these spectra were chosen due to their high signal-to-noise ratio and we felt they represented the various states of AG Dra.

The overall variability of AG Draconis is of considerable interest. Since we are only showing representative UV spectra, the temporal variability of AG Dra is shown in Figures 7a–7f, where the line fluxes are plotted as a function of time (Julian Date). The line fluxes are shown in order of increasing wavelength and represent temporal variations of representative ions, N v, O i, O iv], C iv, He ii and O iii]. Many of the He ii fluxes are lower limits since during the outburst phase He ii was saturated. We have indicated with arrows the time of the

1980–1981 and 1985–1986 outbursts. Note the close correlation of the maxima of the line fluxes with the occurrence of the outbursts which is apparent for ions of wide ionization stages from N v λλ1238, 1242 to O i λλ1302–1306. The uncertainties in the line fluxes are higher in these plots, since the data span nearly a decade and the mean sensitivity degradation in the SWP camera is ~1% per year (Bohlin & Grillmair 1988). This would lead to maximum uncertainties of ~10% in the emission lines from 1979 June to 1989 November.

Finally, in Figures 8a–8e we show emission line N v, O i, O iv], N iv], and O iii] fluxes plotted as a function of the C iv flux. One feature clearly emerges here: line fluxes are, in general, proportional to the C iv flux for a variety of states of

TABLE 3B

HIGH-RESOLUTION LWR/LWP λλ2000–3200 SPECTRA OF AG DRACONIS

| Ion | LWR 12124 ACTIVE | | LWP 5514 ACTIVE | | LWP 16674 QUIESCENT | |
|---|---|---|---|---|---|---|
| | λ(IUE) (Å) | Absolute Flux[a] | λ(IUE) (Å) | Absolute Flux[a] | λ(IUE) (Å) | Absolute Flux[a] |
| [O ii] ...... | 2470.56 | 0.4 | ... | ... | ... | ... |
| He ii ...... | 2509.78 | 3.6 | 2509.92 | 3.2 | 2510.96 | 0.4 |
| Mg ii ...... | 2794.20 | 4.9 | 2794.33 | 3.8 | 2794.34 | 1.8 |
| Mg ii ...... | 2801.30 | 3.0 | 2801.54 | 2.3 | 2801.45 | 1.0 |
| O iii ....... | 3119.98 | 3.3 | 3120.08 | 1.8 | 3120.26 | 0.1 |
| O iii ....... | 3131.17 | 6.7 | 3131.35 | 5.0 | 3131.48 | 0.7 |
| He ii ...... | 3201.12 | 7.9 | 3201.43 | 13.4 | 3201.54 | 1.5 |

[a] Fluxes are in units of $10^{-12}$ ergs cm$^{-2}$ s$^{-1}$.

ACTIVE

N V

N V

SWP 15710

ABSOLUTE FLUX (Erg/cm² s A)

WAVELENGTH (A)

QUIESCENT

N V

N V

SWP 20162

ABSOLUTE FLUX (Erg/cm² s A)

WAVELENGTH (A)
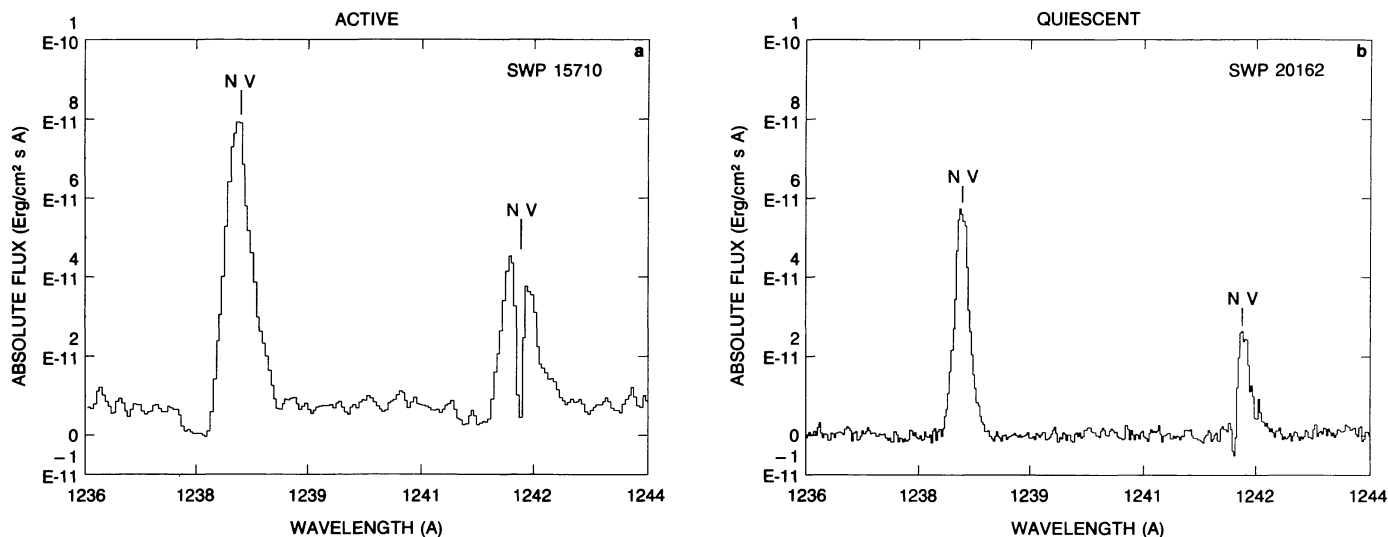
FIG. 2.—High-resolution N v λλ1238.8, 1242.8 spectra observed in AG Dra during (*a*) an active phase (1981 December) and (*b*) a quiescent (1983 June) phase. Note the P Cygni profiles and the double-peaked λ1242.8 emission line in Fig. 2*a* (SWP 15710). The red component of the doublet in Fig. 2*b* is affected by the presence of a reseau.

ACTIVE

O IV]

SWP 25444

Si IV

O IV]

O IV] + Si IV

Si IV

O IV]

ABSOLUTE FLUX (Erg/cm² s A)

WAVELENGTH (A)

QUIESCENT

O IV]

SWP 20162

Si IV

O IV]

O IV] + Si IV

Si IV

O IV]

ABSOLUTE FLUX (Erg/cm² s A)

WAVELENGTH (A)
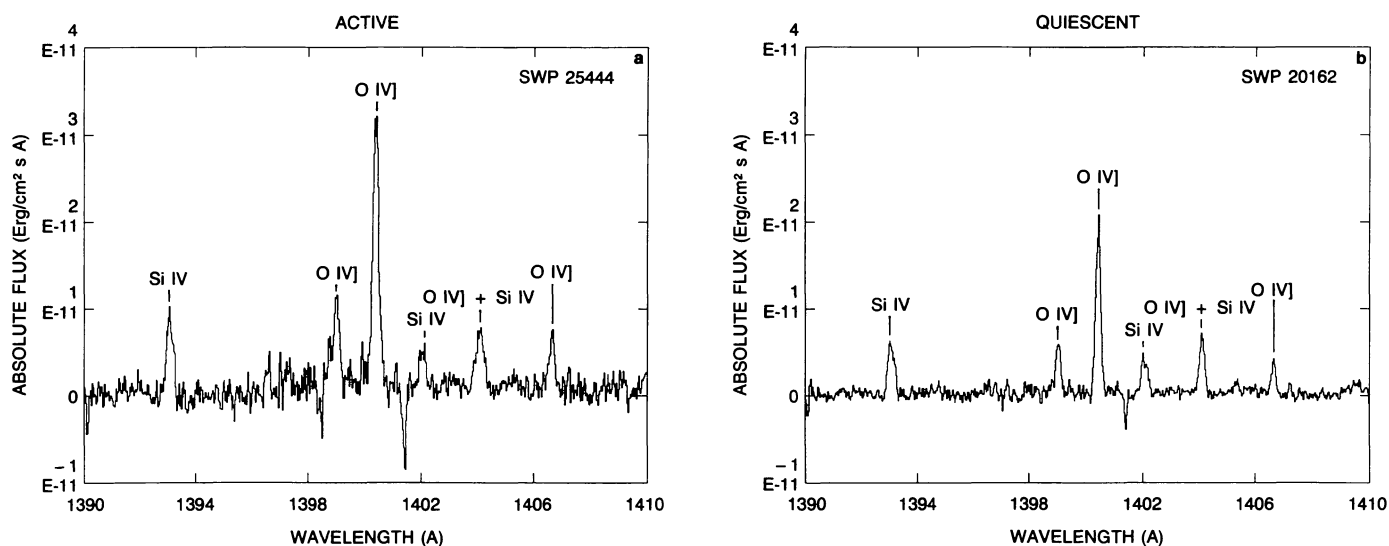
FIG. 3.—High-resolution Si IV and O IV] (λλ1394–1407) emission line spectra in AG Dra. Fig. 3*a* represents activity (1985 March), and Fig. 3*b* was taken in quiescence (1983 June)

ACTIVE

C IV

C IV

SWP 25444

ABSOLUTE FLUX (Erg/cm² s A)

WAVELENGTH (A)

QUIESCENT

C IV

C IV

SWP 20162

ABSOLUTE FLUX (Erg/cm² s A)

WAVELENGTH (A)
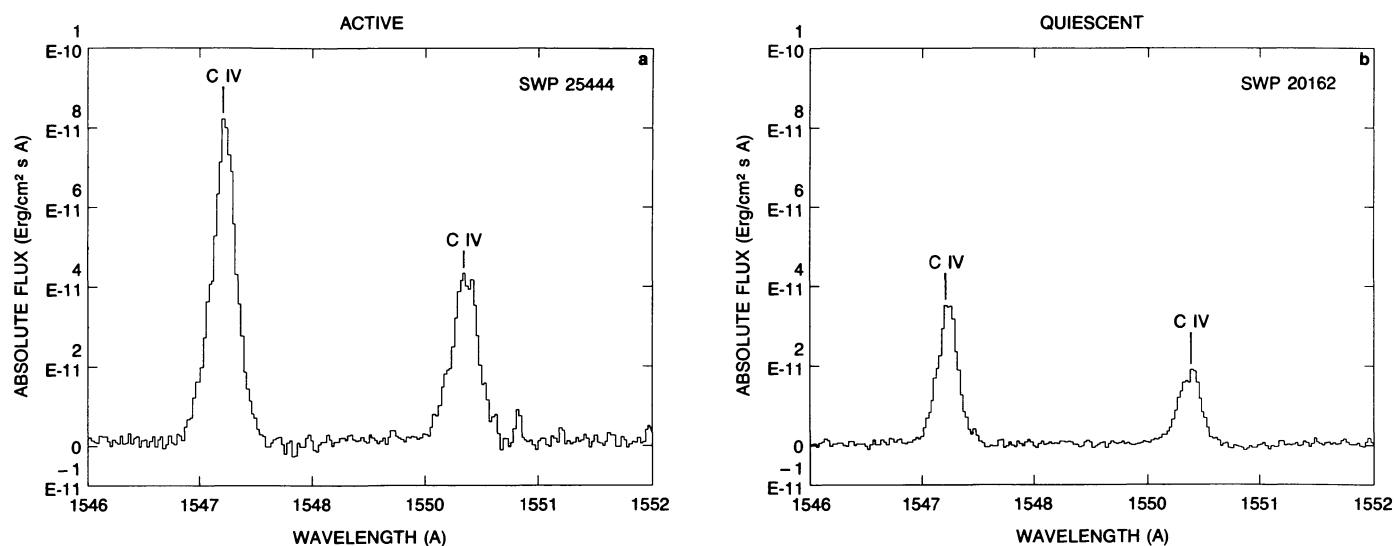
FIG. 4.—High-resolution C IV λλ1548.8, 1550.8 doublet in AG Dra observed in (*a*) an active state (1985 March) and (*b*) a quiescent state (1983 June)
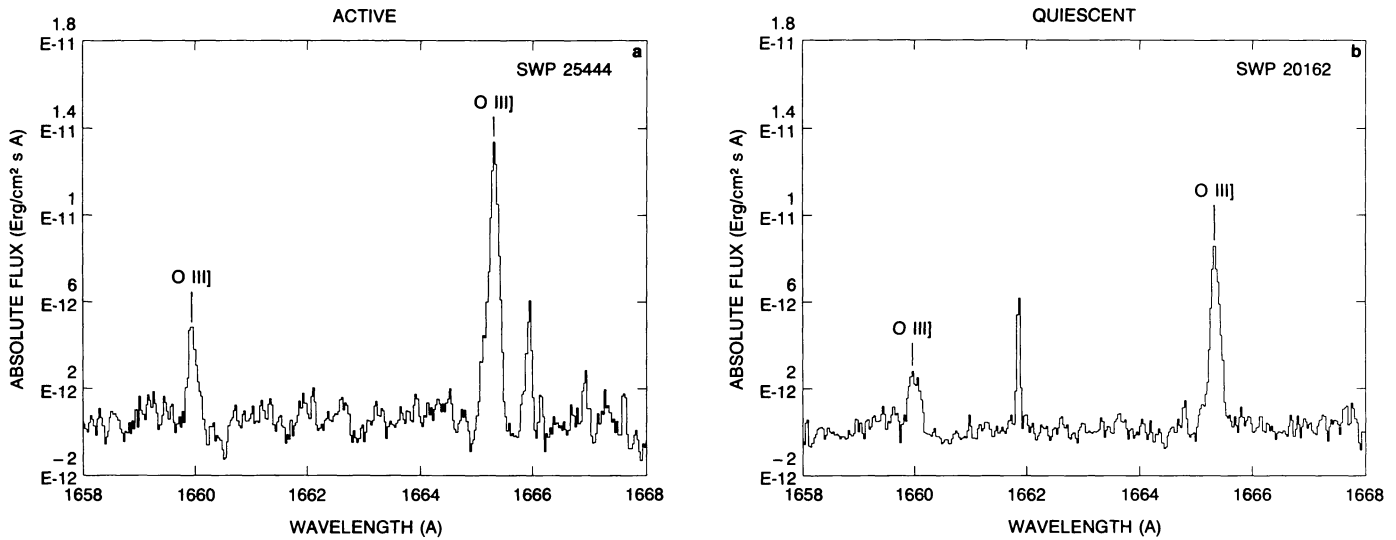
FIG. 5.—High-resolution O III] λλ1660.8, 1666.2 spectra shown in AG Dra during (*a*) activity (1985 March) and (*b*) quiescence (1983 June)

the system in quiescence (*circles*) and in outburst (*triangles*) when the line fluxes are low. There is an interesting feature discerned from this figure. There is a gap in the C IV fluxes for values in the range $20-40 \times 10^{-12}$ ergs cm$^{-2}$ s$^{-1}$ as well as a less prominent gap in the N V fluxes for values in the range $25-35 \times 10^{-12}$ ergs cm$^{-2}$ s$^{-1}$ and possibly in N IV]. In outburst, however, the overall dependence tends to saturate for O I and O III] for values of C IV above $40 \times 10^{-12}$. This would indicate that when C IV is above a certain value, we then are observing regions closer to the hot star where C IV is emitted. One possible interpretation of the gap in the C IV and N V fluxes as well as the above mentioned saturation is that there is a distinct region near the hot component formed during the outburst. During quiescence or low-flux outburst states, we are observing lower density regions further away from the hot source.

## 3. DATA ANALYSIS

The results of UV observations and analysis are described in this section. The associated nebular, stellar, and possible accretion disk parameters are presented.

### 3.1. *UV Lines and Continuum*

As shown in Figures 1*a*–1*h*, the UV spectra of AG Dra are dominated by intense resonance and weak intersystem emission lines, with the primary emission arising from spectral lines with ionization potentials greater than 30 eV. We shall discuss the presence of strong permitted emission lines, the general weakness or absence of the semi-forbidden lines and the overall shape of the UV continuum.

The SWP spectral range λλ1200–2000 clearly shows the UV
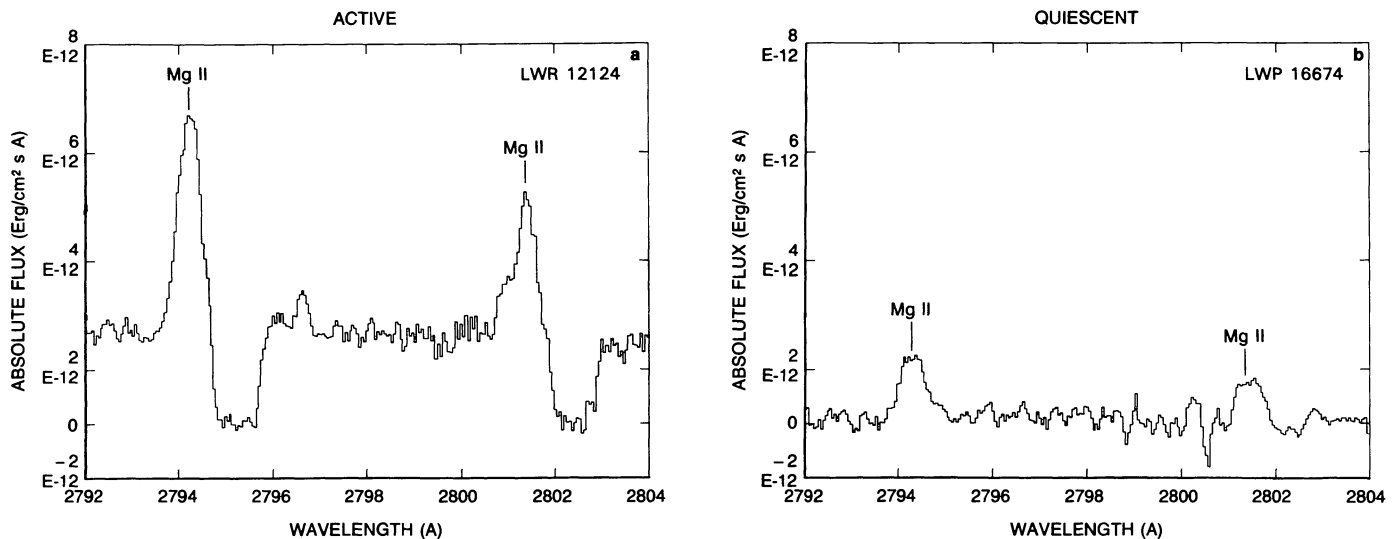


FIG. 6.—High-resolution Mg II λλ2795.5, 2802.6 observed in AG Dra in (*a*) an active phase (1981 December) and (*b*) a quiescent phase (1989 October). Note the broad apparent inverse P Cygni profile in Fig. 6*a* (LWR 12124).
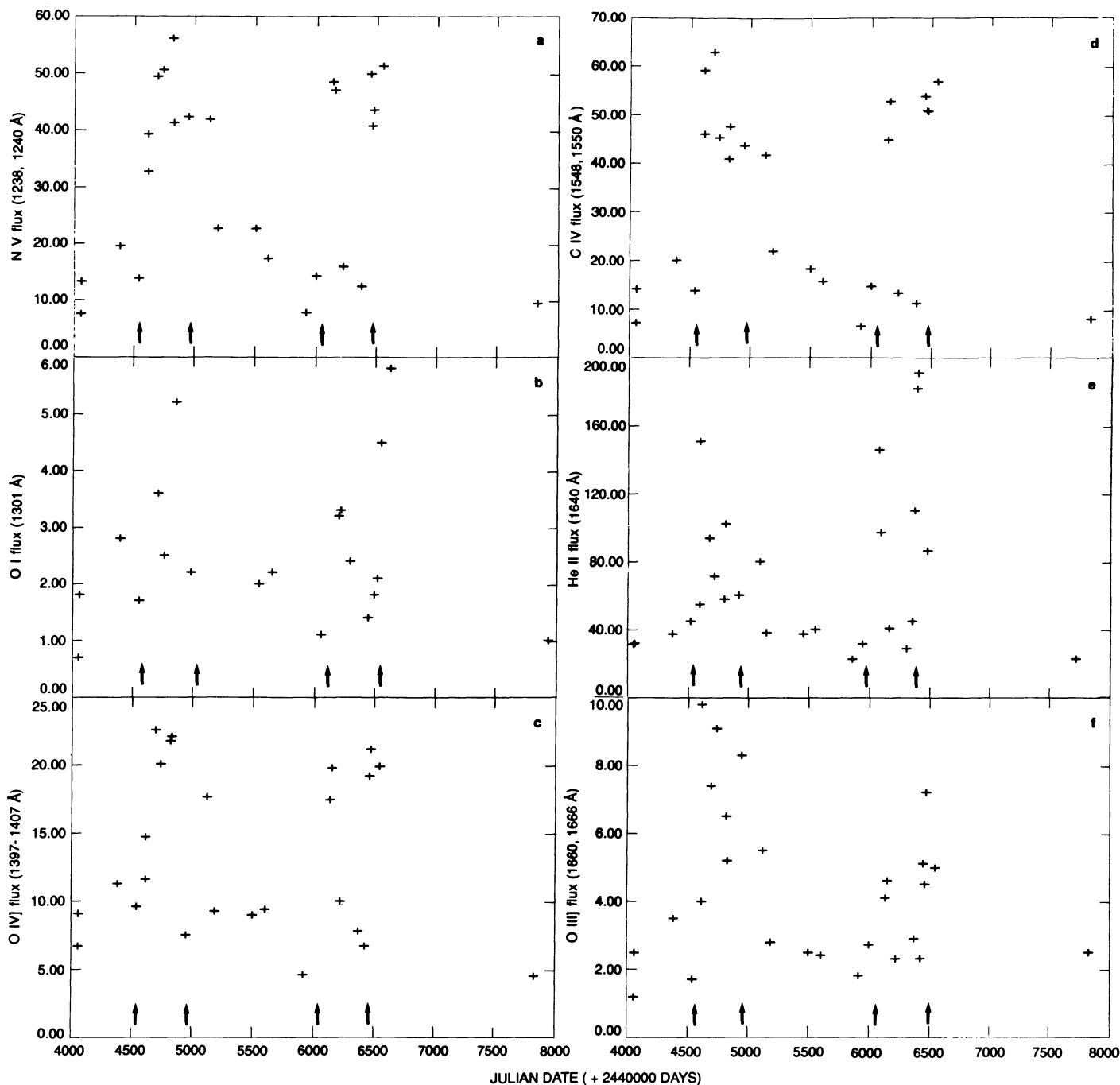
FIG. 7.—(a) N v λλ1238, 1242, (b) O I λλ1302–1306, (c) O IV] λλ1397–1407, (d) C IV λλ1548, 1550, (e) He II λ1640 (often saturated), and (f) O III] λλ1660, 1666 low-resolution absolute fluxes of AG Dra plotted against time (Julian Date). The arrows represent the UV outburst periods of AG Draconis (1980 November–1981 November) and (1985 February–1986 January). Note that the emission line maxima occur between the arrows for both outburst events. Line fluxes are in units of $10^{-12}$ ergs cm$^{-2}$ s$^{-1}$.

continuum flux distribution rising towards shorter wavelengths, consistent with hot stellar blackbody emission. We have fitted the SWP continuum with blackbody curves and have obtained a lower limit to the temperature $T_* \sim 40,000$ K. If, however, we assume that there is a substantial nebular continuum beyond $\sim\lambda1600$ Å (cf. Mürset et al. 1991) and fit only the short wavelength λλ1200–1600 part of the SWP con-

tinuum, we find a higher limit of $T_* \sim 80,000$ K. This agrees with the Zanstra method results (see below).

We find that the UV continuum level was considerably higher in the 1981 outburst (Figs. 1a and 1e) as compared with the 1986 outburst (Figs. 1c and 1g). Viotti et al. (1984) have reported a similar increase in the 1981 continuum. However, the 1986 outburst has not been studied by these authors. N v
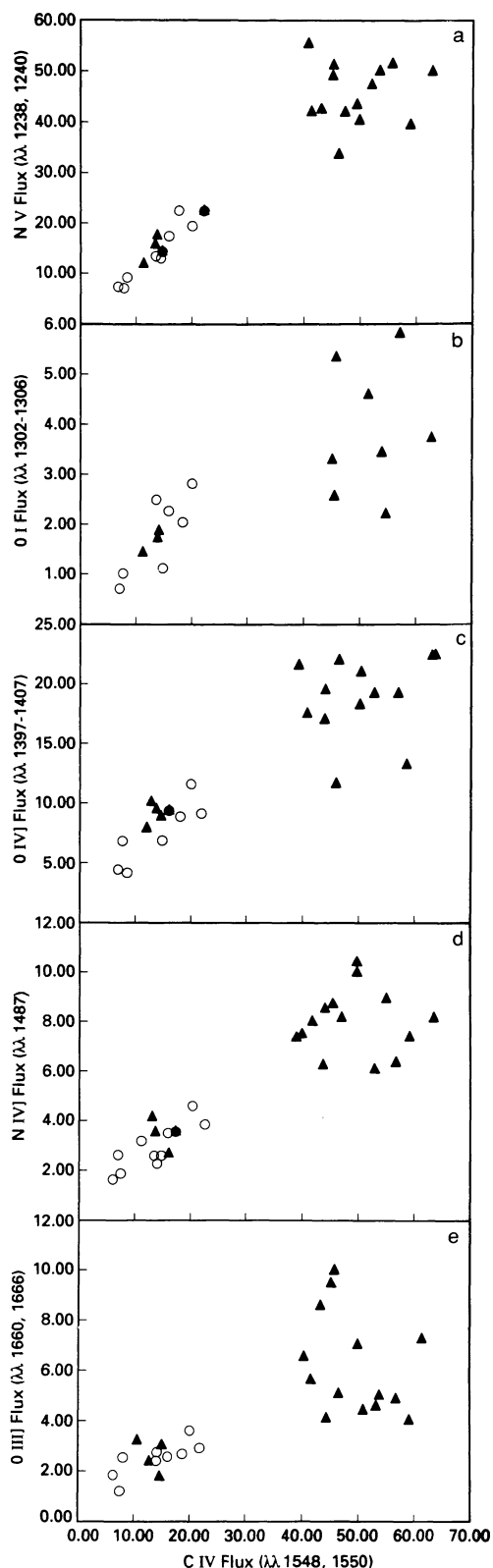
FIG. 8.—(a) N v λλ1238, 1242, (b) O I λλ1302–1306, (c) O IV] λλ1397–1407, (d) N I] λ1487, and (e) O III] λλ1660, 1666 low-resolution absolute fluxes plotted against C IV λλ1548, 1550 absolute flux for AG Dra. The solid triangles represent fluxes taken during the active phases and the circles represent fluxes taken in quiescence. The units of fluxes are $10^{-12}$ ergs cm$^{-2}$ s$^{-1}$.

λλ1238, 1242, C IV λλ1548, 1550 and He II λ1640 are the strongest lines in both active and quiescent states, while Si III] λ1892 and C III] λλ1907, 1909 are very weak in both spectra. The weakness of Si III] and C III] could be due to a high-density nebula surrounding the star, where these semi-forbidden lines are formed. The UV continuum flux distribution noticeably increases towards longer wavelengths in the LWP/LWR λλ2000–3200 wavelength region. He II λλ2358, 2511, 2730 lines are the dominant emission features in the active phase of the star. The weakness of Mg II λλ2795, 2803 during the 1986 January outburst (Fig. 1g) suggests that during the 1986 activity Mg II is being suppressed in some manner. In quiescence, He II drops dramatically, while the Mg II emission lines λλ2795, 2803 (Fig. 1f) become pronounced.

A P Cygni profile is clearly exhibited in the N v λλ1238, 1242 resonance doublet during outburst (Fig. 2a). In Figure 2a (SWP 15710) a P Cygni profile is evident in the λ1238.8 component, we obtained $\Delta v \sim 200$ km s$^{-1}$ which is in agreement with Viotti et al. (1983, 1984) and Lutz et al. (1987). Note the unique, peculiar double profile of the λ1242.8 component in SWP 15710 (Fig. 2a), although this structure may be affected by the presence of a reseau. This may indicate multiple profiles as in the ejection of a shell with a velocity separation $\Delta v \sim 70$ km s$^{-1}$. None of the C IV λλ1548, 1550 doublets in any of the outburst or quiescent phases exhibited P Cygni structure (Fig. 4b).

In Figure 6a (LWR 12124) we show the Mg II λλ2795, 2803 profiles during the 1980/1981 outburst. This is a false inverse P Cygni profile due to the presence of interstellar Mg II absorption features (cf. Viotti et al. 1983; Lutz et al. 1987). Because the Mg II line fluxes were obtained by different cameras at different times, uncertainties in the line intensities could be high $\sim 20\%$–$30\%$.

The doublet N v λλ1238, 1242, C IV λλ1548, 1550, and Mg II λλ2795, 2803 ratios were calculated. C IV and Mg II ratios were found to be near the nebular (optically thin) ratio of 2:1, while the N v doublet ratio ranged from 2 to 4 which is greater than the optically thin ratio of 2:1. This could be the result of the multiple structure of the λ1242.8 component in Figure 2a.

### 3.2. Nebular Parameters

As mentioned before, the UV spectrum of AG Dra is dominated by intense permitted lines and weak semi-forbidden emission lines. We found that the O IV] multiplets were the only semi-forbidden lines which contained enough information to obtain an estimate of the electron density. Following Flower & Nussbaumer (1975), we derived electron densities from the O IV] density-dependent line ratios $I(\lambda1404.81)/I(\lambda1401.16)$ and $I(\lambda1407.39)/I(\lambda1401.16)$. These line intensity ratios imply a density in the range $10^{10} \leq n_e \leq 10^{11}$ cm$^{-3}$. This estimate is higher than most other electron density estimates, $n_e \sim 10^{10}$ cm$^{-3}$ (Viotti et al. 1983; Lutz et al. 1987). The higher densities found here may be the reason for the overall weakness of N III], Si III], and C III]. However, Lutz et al. (1987) has calculated $n_e$ from the Si III] lines, finding much lower densities than those obtained from the O IV] lines (i.e., $10^5$–$10^6$ cm$^{-3}$ vs. $10^{10}$ cm$^{-3}$). In the two aforementioned works an explanation to this feature is given by suggesting a possible "density stratification," or more than one site asso-

ciated with the emission lines. Due to the overall weakness of the Si III] lines we find these estimates unreliable.

The absolute intensities of the UV lines and the electron density can be used to estimate the characteristic length of the nebular emitting region. For densities up to $\sim 5 \times 10^{10}$ cm$^{-3}$ the semi-forbidden line strengths are proportional to $n_e^2 L\Omega$ (Osterbrock 1974), where $L$ is the path length through the emitting region (Kafatos, Michalitsianos, & Feibelman 1982) and $\Omega$ the solid angle of the region. This expression is proportional to $n_e^2 L^3/d^2$ for a spherical region, where $L$ is the size or diameter and $d$ the distance. If the region, however, is in the form of streams, rings, or a disk, we have to take into account the geometrical effects of observation. In general, (Kafatos, Michalitsianos, & Feibelman 1982) we can always write it as $n_e^2 L^3 f_g$, where $f_g < 1$ is a factor depending on the geometry of the region relative to the line of sight and the equality applies in the spherically uniform case. In the general case, $L$ is understood to be the largest characteristic size of the region (e.g., the diameter of the disk, etc.). Since the line intensities are proportional to $n_e^2 L^3 f_g$, if we set $f_g = 1$ and substitute values for $n_e \sim 10^{10}$ cm$^{-3}$, $d = 700$ pc and $T_e \sim 10,000$ K, the resulting values $L \sim 10^{12}$–$10^{13}$ cm should be considered as lower limits. Our choice of the value for $T_e$ has been made on the basis of previous work (Mürset et al. 1991). Also, work by Kenyon & Webbink (1984) and Slovak et al. (1987) leads to $T_e = 10,000$ K and 20,000 K, respectively, which are typical of symbiotic star systems (Nussbaumer 1982). Kaler (1987) also concludes that $T_e$ is no greater than 20,000 K and may be as low as 8000 K.

### 3.3. Properties of the Primary

We used Kepler's law to determine the semi-major axis $a$. Assuming $M_1 \sim 1$–5 $M_\odot$ and $M_2 \sim 1$ $M_\odot$ (Iijima 1987) we calculated $a \sim 1.4 \times 10^{13}$ cm, which is comparable to the emission path-length $L$. We estimate the radius of the primary star $R_1 \sim 1.7 \times 10^{12}$ cm, or $\log(R_1/R_\odot) \sim 1.4$ which according to Allen (1976) corresponds to a K5 III giant for the cool component. Iijima (1987) reports a similar value for $R_1$ of $\log(R_1/R_\odot) \sim 2.4$. The spectral classification of the primary as a K star and an extinction of $E_{B-V} = 0.06$ corresponds to a distance $d_{pc} = 700$ pc (Anderson et al. 1981; Mürset et al. 1991). The apparent and absolute magnitudes are $m_v \sim 9.44$ (Kenyon 1986) and $M_v \sim 0.03$, respectively.

### 3.4. Properties of the Secondary

We calculated the number of ionizing photons using the Stromgren relation. With assumed values of $n_e \sim 10^{10}$ cm$^{-3}$ and $T_e = 10,000$ K we find the number of hydrogen ionizing photons or Lyman continuum photons, $N_i(\text{H I}) \equiv N_i(h\nu \geq 13.6 \text{ eV}) \sim 1.0 \times 10^{46}$ s$^{-1}$ for the active state of the star and $N_i(\text{H I}) \sim 4.4 \times 10^{45}$ s$^{-1}$ for quiescence. The results of Hummer & Mihalas (1970) show that the overall number of ionizing (beyond the Lyman limit) photons in their stellar models is not greatly different from the estimated number of photons that arise from a blackbody. We then used the blackbody formula (Allen 1976) to estimate $R_*$ and $L_*$, the radius and luminosity of the secondary hot star. These values will allow us to find out if the size and luminosity of the secondary is consistent with the number of ionizing photons $N_i(\text{H I})$ required to photoionize the nebula. Table 4 gives these values at different effective temperatures ($T_* = 50,000$ K, 100,000 K, and 200,000 K) in the active and quiescent phases of the star. In all cases the hot component falls within the central stars of planetary nebulae region of the H-R diagram (cf. Kafatos, Michalitsianos, & Hobbs 1980).

The theoretical results found in Tables 4 and 5 are subject to *IUE* uncertainties since the absolute emission line flux is affected by the calibration errors and signal-to-noise ratio. The estimate for the size of the nebular emitting region $L$ is obtained from the observed emission line intensities. These line intensities are subject to uncertainties of $\sim 20\%$ for the strongest lines and higher for the weaker lines when taking into account the sources of error mentioned above. The size $L$ is then used to obtain an estimate of the number of ionizing photons from the Stromgren relationship, which results in large uncertainties (since the relative errors are related by $\Delta N_i/N_i = 3\,\Delta L/L$) for $N_i$. Therefore, the values in Tables 4 and 5 should be taken as estimates to within a factor of 3–5 of what the properties of ionizing source may be.

Kenyon & Webbink (1984) found $R_* = 0.014$ $R_\odot$ during quiescence and 2–3 times greater during the 1980 outburst and $T_* \sim 166,000$ K. These authors consider the hot star very likely to be a white dwarf. Iijima (1987), on the other hand, found a radius $R_* = 0.02$ $R_\odot$ with a corresponding temperature $T_* \sim 150,000$ K. Finally, Mürset et al. (1991) give values of $R_*$ at four different times, between 1979 September and 1985 June. These vary periodically between $R_* = 0.01$ $R_\odot$ ($T_* = $

### TABLE 4
HOT COMPONENT PARAMETERS OF AG DRACONIS FOR ASSUMED
EFFECTIVE TEMPERATURES $T_*$

|  | VALUE | | |
|---|---|---|---|
| PARAMETER | ($T_* = 50,000$ K) | ($T_* = 100,000$ K) | ($T_* = 150,000$ K) |
| Active | | | |
| $R_*$ ($R_\odot$) | 0.2 | 0.04 | 0.01 |
| $L_*$ ($L_\odot$) | 147.0 | 133.8 | 210.0 |
| Quiescent | | | |
| $R_*$ ($R_\odot$) | 0.1 | 0.03 | 0.01 |
| $L_*$ ($L_\odot$) | 68.0 | 62.0 | 97.0 |

TABLE 5
ACCRETION DISK PARAMETERS FOR AG DRACONIS

| Parameter | Active | Quiescent |
|---|---|---|
| $T_{\rm bl}$ = 40,000 K | | |
| $R_*$ ($R_\odot$) ............. | 2.4 | 1.6 |
| $\dot{M}_{-8}$ ($M_\odot$ yr$^{-1}$) ...... | $2.0 \times 10^{-5}$ | $5.9 \times 10^{-6}$ |
| $L_d$ ($L_\odot$) ............. | 127.0 | 55.9 |
| $L_T/L_{\rm Edd}$ ............ | $1.0 \times 10^{-2}$ | $4.4 \times 10^{-3}$ |
| $T_{\rm bl}$ = 100,000 K | | |
| $R_*$ ($R_\odot$) ............. | 0.3 | 0.2 |
| $\dot{M}_{-8}$ ($M_\odot$ yr$^{-1}$) ...... | $1.7 \times 10^{-6}$ | $5.1 \times 10^{-7}$ |
| $L_d$ ($L_\odot$) ............. | 84.4 | 37.1 |
| $L_T/L_{\rm Edd}$ ............ | $7.0 \times 10^{-3}$ | $3.1 \times 10^{-3}$ |

105,000 K) and $R_* = 0.009\, R_\odot$ ($T_* = 125,000$ K), with similar periodic variations in luminosity: $L_* = 10\, L_\odot$ in 1979 September to $L_* = 19\, L_\odot$ in 1985 June. Mürset et al. (1991) found that temperatures and luminosities obtained shortly after an outburst are higher than those obtained after a longer quiescence phase. Our values of $R_*$ and $L_*$ found here are consistent with previous estimates if indeed the temperature of the hot secondary is $\geq 10^5$ K.

We have used the modified Zanstra method for He II $\lambda1640$ to estimate the effective temperature of the hot component. In this method the line intensity is divided by the continuum (assumed stellar) at the same wavelength (cf. Pottasch 1984). We find that $T_* \geq 87,000$ K during quiescence, in general agreement with Mürset et al. (1991). This is a lower limit since part of the continuum at $\lambda1640$ must be nebular. In fact, as Mürset et al. (1991) point out, the Zanstra method fails during outburst because of substantial contribution from the nebular continuum being present in the SWP region of the spectrum. The Bowen resonance-fluorescence line of O III $\lambda3132.9$ can also be used to estimate the number of photons below 228 Å [the He II Lyman continuum photons, $N_i$(He II) $\equiv N_i$(h$\nu \geq$ 54.4 eV)]. The O III line contributes $\sim 0.31$ of the total fluorescence line flux (Osterbrock 1989). Moreover, the overall fraction of He II Ly$\alpha$ photons converted into Bowen resonance-fluorescence photons is $\sim 0.5$ (Osterbrock 1989). Since the nebula is thick in the He II Lyman lines, recombinations of He II to all levels $n > 2$ yield the number of He II Ly$\alpha$ photons (Seaton 1960). The observed $\lambda3132.9$ flux, therefore, implies that $N_i$(He II) $\sim 3.2 \times 10^{43}$ s$^{-1}$ for active times and $N_i$(He II) $\sim 8.7 \times 10^{42}$ s$^{-1}$ for quiescence.

From the number of ionizing hydrogen photons produced $N_i$(H I) and the number of He II Lyman continuum photons $N_i$(He II), we can estimate the temperature of the blackbody by taking the ratio of $N_i$(H I)/$N_i$(He II). During outburst we calculate $N_i$(H I)/$N_i$(He II) $\sim 0.0032$, and a corresponding temperature of $T_* \sim 43,000$ K. The ratio during quiescence is $\sim 0.0020$, which corresponds to a temperature of $\sim 37,000$ K. These are, however, uncertain due to the uncertainties in the O III $\lambda3132.9$ fluxes being in a less sensitive part of the LWP detector. The estimates of $T_*$ found in the present work by using the modified Zanstra method are not in disagreement with the higher temperatures of $T_* \sim 10^5$ K reported else-

where, e.g., Kenyon & Webbink (1984), Lutz et al. (1987), and by Mürset et al. (1991).

### 3.5. Accretion Disk Parameters

Alternatively, the photoionizing radiation may be due to the presence of an accretion disk. We assume here that the observed blackbody continuum arises from the boundary-layer accretion disk around the secondary star with a temperature $T_{\rm bl}$. In what follows we adopt different values of $T_{\rm bl}$.

#### 3.5.1. $T_{\rm bl} = 40,000$ K Lower-Limit (This Work)

For this temperature, the corresponding relationships are

$$R_* \geq 52.9[N_i(\text{H I})/10^{45}\,\text{s}^{-1}]^{1/2} \times 10^9 \text{ cm} ,$$

$$\dot{M}_{-8}M_* \geq 63.5[N_i(\text{H I})/10^{45}]^{3/2} ,$$

$$L_d \geq 12.7[N_i(\text{H I})/10^{45}]L_\odot ,$$

$$L_T/L_{\rm Edd} \geq 1.0 \times 10^{-3}M_*^{1}[N_i(\text{H I})/10^{45}] ,$$

where $R_*$ is, again, the radius of the secondary, $\dot{M}_{-8} = M/10^{-8}$ $M_\odot$ yr$^{-1}$ is the accretion rate, $M_*$ is the mass of secondary in solar masses, $L_d$ is the luminosity of the disk, and $L_T$ is the total luminosity (disk + boundary layer, assuming that $L_d = L_{\rm bl}$ (cf. Kafatos, Michalitsianos, & Fahey 1985).

#### 3.5.2. $T_{\rm bl} = 100,000$ K (cf. Mürset et al. 1991, and This Work).

For this temperature, the corresponding relationships are

$$R_* \geq 6.9[N_i(\text{H I})/10^{45}]^{1/2} \times 10^9 \text{ cm} ,$$

$$\dot{M}_{-8}M_* \geq 5.5\,[N_i(\text{H I})/10^{45}]^{3/2} ,$$

$$L_d \geq 8.44[N_i(\text{H I})/10^{45}]L_\odot ,$$

$$L_T/L_{\rm Edd} \geq 7.07 \times 10^{-4}\,M_*^{1}(N_i(\text{H I})/10^{45}) .$$

Assuming $M_* = 1$ and the (average) values

$$N_i(\text{H I}) = 10^{46} \text{ s}^{-1} \quad \text{(active phase)} ,$$

$$N_i(\text{H I}) = 4.4 \times 10^{45} \text{ s}^{-1} \quad \text{(quiescent phase)} ,$$

we obtain the results shown in Table 5. The lower limits are applicable if the ionized region is particle bound. Otherwise the equality sign applies.

It is unlikely that the secondary star in AG Dra is a main-sequence–type star (solar-type) star. The only other candidate for the presence of such secondary is CI Cygni and the properties of AG Dra are markedly different from CI Cygni. We, therefore, discard the case $T_{\rm bl} = 40,000$ K. If, on the other hand, $T_{\rm bl} = 100,000$ K, we find that the secondary is a subdwarf and 10 times larger than the size estimated if the source of the photoionizing flux was the hot subdwarf rather than the boundary layer of an accretion disk. It may be that the two values of $R_*$ during the active and quiescent phase are different (for constant $T_{\rm bl}$) because in the accretion disk scenario as-

sumed here the effective photosphere where the disk ends is larger during outburst.

## 4. DISCUSSION AND CONCLUSIONS

The overall linear dependence of the line fluxes in quiescence when plotted versus C IV λλ1548, 1550 (see Fig. 8) argues that all UV lines originate in similar spatial regions surrounding the star. During outburst, we may be observing higher density regions which shine in, primarily, high-ionization states like C IV and N V. In general, if other ions were not spatially coincident with C IV, one would not have expected a linear dependence of the fluxes. The detailed analysis presented below argues for rather small variations of $L$ obtained e.g., $L \sim 7-9 \times 10^{12}$ cm for the intermediate to high-ionization state ions; this reinforces our interpretation that the linear behavior of the flux-flux plots argue for emission in similar regions. In outburst, however, the linear dependence is not as prominent.

We have analyzed the strongest UV emission lines of AG Dra from 1979–1989 period and calculated the relative ionic abundances for the ions with strong UV lines. The time evolution of these ionic abundances through the quiescent and active phases of the symbiotic star may shed some light on the nature of the outburst phenomenon for this object and symbiotic stars in general.

Recently, Nussbaumer et al. (1988) have calculated elemental C/N and O/N abundance ratios for 24 symbiotics, including AG Dra, and have found common properties in all the nebulae. In order to find the ionic abundances from the observed line fluxes we have followed a procedure similar to Kafatos, Michalitsianos, & Hollis (1986). For collisionally excited lines, the abundance of an ion $A_z$, of element A in ionization stage $Z$, depends on the dereddened line flux, $F$, the electron temperature, $T_e$, the electron density, $n_e$, the line excitation energy, $\Delta E$, the distance of the hot star from Earth, $d$, the nebular size $L$, and the chemical abundances prevalent in the ionized nebula, $n_A$ compared to solar values, $n_{A\odot}$, in the following manner:

$$N_{A,Z} \propto FT_e^{1/2} \exp{(\Delta E/kT_e)}(n_e^2 L^3)^{-1} d^2 (n_A/n_{A\odot})^{-1} \quad (1)$$

where a spherical nebular shape has been assumed and the region's solid angle has been set equal to $L^2/d^2$, or $f_g = 1$. (Kafatos et al. 1980). Furthermore, we have assumed solar abundances.

Assuming $d = 700$ pc, $E_{B-V} = 0.06$ (Viotti et al. 1983), and the values of $n_e = 3 \times 10^{10}$ cm$^{-3}$ and $T_e = 10^4$ K, we applied equation (1) to the ions whose lines are present in a given LORES spectral image and determined a size $L$ for all of the available ionization stages of a given element. We proceeded in this manner with all the LORES SWP and LWP/LWR spectral images that were available, thus covering all the individual dates in the 1979–1989 period. The values of $L$ are lower limits because not all possible ionization stages emit lines in the far-UV and not all observable *IUE* lines had acceptable S/N ratios.

The next step was to assign more realistic values of $L$ to each specific ion, bearing in mind the possible "stratification" of the nebula, as described by Dyson & Williams (1980) for all

photoionized nebulae in general and for the particular case of AG Dra (e.g., Lutz et al. 1987; Friedjung 1988). We assumed that ions with similar ionization potentials are likely to be formed in the same nebular region. Therefore, we classified the ions under study by their ionization potentials and grouped them together. We then assigned the same value of the scale size $L$ to all the ions in the same group.

The value of the size $L$ assigned to each individual group, on a given observation date, was the arithmetic mean of the lower limit estimates for $L$. In general, the values of the scale size $L$ vary by not more than a factor of $\sim 2$ between the most extreme cases of high-ionization stages (N v) and low-ionization stages (C II). For example, in the outburst spectrum SWP 13955 we found the corresponding values of the scale size $L$: for N v, $9.28 \times 10^{12}$ cm; for N IV, O IV, and He II, $7.94 \times 10^{12}$ cm; for C IV and O III, $7.04 \times 10^{12}$ cm; for C III, N III, and Si IV, $7.48 \times 10^{12}$ cm; and finally for Si III, O II, and C II $3.78 \times 10^{12}$ cm.

Again assuming solar/cosmic abundances, we present a plot (Fig. 9) of the normalized abundances of N v, N IV, N III versus time (Julian Date). Lines from the ions shown in Figure 9 are strong and were present in most of the available images. The arrows shown in each figure represent the UV flux maximum (Kaler 1987) of the binary phase and the brackets represent the 1980–1981, 1985–1986 outbursts. We applied Meinunger's (1979) ephemeris for the apparent magnitude in the UV, Max (U) = JD 2438900 + 554$E$, to find the Julian Dates at which maxima and minima in the binary phase will occur (see Table 6). The maxima and minima of the normalized abundances generally follow those of the binary phases in both of the two overlapped outbursts, 1980 November to 1981 November and 1985 February to 1986 January: the ionic abundances achieve extrema (maximum or minimum) during the two outburst events and closely correlate with the binary
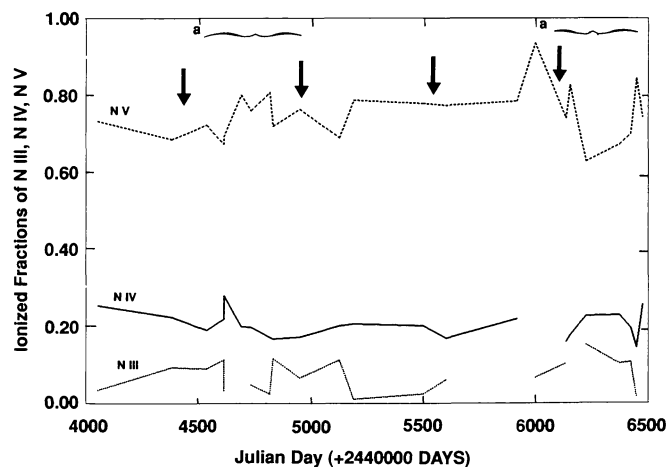


FIG. 9.—Ionized fractions of N v, N IV, and N III plotted against time (Julian Date) for AG Dra. N v (*top*) is the dashed line, N IV (*middle*) is the solid line, and N III (*bottom*) is the dotted line. The arrows represent the maxima of the binary phase according to Meinunger (1979). The brackets correspond to the outburst events of AG Dra (1980 November–1981 November) and (1985 February–1986 January). Where lines are broken, the absolute line intensities were not available, the spectra were saturated or the spectra had unacceptable signal-to-noise ratios.

TABLE 6

The Maxima and Minima of AG Draconis Calculated for the Binary Phase

| Orbital Phase | Julian Date | Orbital Phase | Julian Date | State of System | Julian Date (+2440000 days) |
|---------|---------|---------|---------|---------|---------|
| Maximum | 2444400 | Minimum | 2444700 | Quiescent | ~3800–4500 |
| Maximum | 2445000 | Minimum | 2445200 | Active | ~4500–4900 |
| Maximum | 2445500 | Minimum | 2445800 | Quiescent | ~4900–6100 |
| Maximum | 2446100 | Minimum | 2446300 | Active | ~6100–6500 |
| Maximum | 2446600 | Minimum | 2446900 | Quiescent | ~6500–7800 |

phase. This would indicate that the ionic abundances respond to the overall orbital motion of the star which itself may be triggering the outbursts. There seems to be no indication of a thermonuclear runaway from the present analysis.

The hot component blackbody continuum is absent during quiescence. This could indicate that in outburst the underlying hot star is exposed, or alternatively, that we are observing the inner regions of an accretion disk that is formed at that time. However, Kenyon & Webbink (1984) interpret the 1980–1981 outburst of AG Dra as having been powered by a thermonuclear runaway event. Iijima (1987) considers the likelihood of a spherically symmetric mass accretion shell being formed around the massive (white dwarf) hot component, which is ejected during outburst episodes with rapidly higher rates accompanied by mild hydrogen flashes. However, Slovak et al. (1987), as well as Lutz et al. (1987) relate the emission lines to the presence of both an accretion disk and an ionized portion of the stellar wind from the cool giant primary. More recently, Friedjung (1988), does not favor the thermonuclear runaway model for AG Dra, on the basis of insufficient model calculations.

Iijima (1987) found a mass accretion rate onto the hot component of about $10^{-7}\ M_\odot\ \mathrm{yr}^{-1}$, much higher than the mass-loss rate from K-type giants. He concludes that it is quite possible that the cool component has an extended atmosphere that fills its Roche lobe. Mürset et al. (1991) also report a mass loss of $\sim 10^{-7}\ M_\odot\ \mathrm{yr}^{-1}$ during quiescent phases. Lutz et al. (1987) claim that the K star does not come close to overfilling its Roche lobe, but if the hot companion has an accretion disk, the mass of the disk comes from accumulation of the wind from the cool star.

The spectral variations of AG Dra in the UV may support a binary model in which the UV variations are due to periodic occultations of an extended photoionized region by the cool star, superposed on large-amplitude variations caused by the activity of the hot source (Viotti et al. 1984). Moreover, Viotti et al. (1984), suggested that the extended hot region could be the upper atmosphere and/or the inner wind of the cool star heated by the radiation of the hot companion. An intense warm wind probably produced by the cool star maybe present in AG Dra (as indicated by the presence of P Cygni profiles in N v), and part of it is probably accreted by the unseen companion, causing the complex phenomenology of AG Dra. The cool star itself could be peculiar by having a stellar wind more intense than that observed in other K stars, and probably an extended chromosphere and transition region (Viotti et al. 1984). The physics of the accretion process, temperature, and instability of the accretion region (or disk) are still unknown,

mainly because of the lack of fundamental physical data on AG Dra which may be derived only from contemporaneous observations at all wavelengths (Viotti et al. 1984).

Even in the absence of contemporaneous observations at all wavelengths, we still can distinguish between (i) a thermonuclear runaway model and (ii) an accretion outburst model.

First of all, it suffices to say that either analysis for the hot star parameters (§ 3.4 and 3.5) yields a hot subdwarf. If an accretion disk is present, the hot subdwarf is larger in radius (Table 5) than in the case when the hot star is the only ionizing source (Table 4). The lack of high velocities in the observed UV lines over the entire time scale of observations argues that mass loss occurs not very near the hot star. We would have expected that high velocities (even for $R_* = 0.31\ R_\odot$, $V_{\mathrm{esc}} \sim 780\ \mathrm{km\ s}^{-1}$) should be present in the UV lines, and that higher velocities should be associated with higher degree of ionization. Since this is not the case, we conclude that no concrete evidence for thermonuclear runaway is present in any of the velocity profiles. Outflow velocities in N v are present, $V \sim 40\ \mathrm{km\ s}^{-1}$ which can rise to a high value of $\sim 200\ \mathrm{km\ s}^{-1}$ during outburst. The N v profiles give evidence of hot outflow material in slow outburst.

Moreover, the strange coincidence of an outburst period with $\sim 3$ times binary period argues for some beating mechanism of ejection tied to binarity. One would not expect that thermonuclear outbursts to be so closely tied to the binary orbit. Ejection from the outward regions of an accretion disk or, alternatively, from the extended atmosphere of the giant should, on the other hand, be expected to be closely tied to the binarity of the system.

Also, the small time scale between outbursts ($\sim 4.5$ yr) argues against thermonuclear runaways. The results of Livio (1986) indicate that high rates of mass transfer and/or masses of the white dwarf near the Chandrasekhar limit are required. Assuming $R_* \sim 0.03\ R_\odot$ for the white dwarf (see Table 4), would require a mass accretion rate of $M \sim 3.7 \times 10^{-3}\ M_\odot\ \mathrm{yr}^{-1}$. Even if $R_* \sim 0.01\ R_\odot$ (cf. Kenyon & Webbink 1984; Mürset et al. 1991) we find that an accretion rate of $M \sim 4.5 \times 10^{-5}\ M_\odot\ \mathrm{yr}^{-1}$ is required (cf. Livio 1986). These accretion rates are too large and would in themselves suppress any thermonuclear runaways. The only viable mechanism for outbursts is tied to the accretion process, possibly due to disk instabilities (Livio 1986).

It is clear that HIRES observations of AG Dra (from the *Hubble Space Telescope*) over extended periods including an outburst phase and contemporaneous coverage at X-rays, UV, and optical wavelengths are needed for understanding of the complex accretion process in this star.

## REFERENCES

Allen, C. W. 1976, Astrophysical Quantities (London: Athlone).
Altamore, A., Baratta, G. B., Cassatella, A., Gionegrando, A., Ponz, D., Ricardi, O., & Viotti, R. 1982, in IAU Colloq. 70, The Nature of Symbiotic Stars, ed. M. Friedjung & R. Viotti (Dordrecht: Reidel), 43
Anderson, C. M., Cassinelli, J. P., & Sanders, W. T. 1981, ApJ, 247, L127
Bohlin, R. C., & Grillmair, C. J. 1988, ApJS, 66, 209
Cassatella, A., Cordova, F. A., Friedjung, M., Kenyon, S. J., Piro, L., & Viotti, R. 1987, Ap&SS, 131, 763
Dyson, J. E., & Williams, D. A. 1980, Physics of the Interstellar Medium (NY: Wiley)
Flower, D. R., & Nussbaumer, H. 1975, A&A, 45, 145
Friedjung, M. 1988, in The Symbiotic Phenomenon, ed. J. Mikolajewska, M. Friedjung, S. J. Kenyon, & R. Viotti (Dordrecht: Reidel), 199
Huang, C. C. 1982, in IAU Colloq. 70, in The Nature of Symbiotic Stars, ed. M. Friedjung & R. Viotti (Dordrecht: Reidel), 185
Hummer, D. G., & Mihalas, D. 1970, MNRAS, 147, 339
Iijima, T. 1987, Ap&SS, 131, 759
Janssen, E. M., & Vyssofsky, A. N. 1943, PASP, 55, 224
Kafatos, M., Michalitsianos, A. G., & Fahey, R. P. 1985, ApJS, 59, 785
Kafatos, M., Michalitsianos, A. G., & Feibelman, W. A. 1982, ApJ, 257, 204
Kafatos, M., Michalitsianos, A. G., & Hobbs, R. W. 1980, ApJ, 240, 114
Kafatos, M., Michalitsianos, A. G., & Hollis, J. M. 1986, ApJ, 62, 853
Kaler, J. B. 1987, AJ, 94, 452
Kaler, J. B., et al. 1987, AJ, 94, 437
Kenyon, S. J. 1986, The Symbiotic Stars (Cambridge: Cambridge Univ. Press)
Kenyon, S. J., & Fernandez-Castro, T. 1987, ApJ, 93, 938
Kenyon, S. J., & Webbink, R. F. 1984, ApJ, 279, 252
Livio, M. 1986, in Variability of Galactic and Extragalactic X-Ray Sources, ed. A. Treves (Milano: Assoc. per L'Avanz Dell' Astron), 350
Lutz, J. H., & Lutz, T. E. 1981, in Proceedings of the North American Workshop on Symbiotic Stars, ed. R. E. Stencel (Boulder: JILA), 28
Lutz, J. H., Lutz, T. E., Dull, J. D., & Kolb, D. D. 1987, AJ, 94, 463
Meinunger, L. 1979, Inf. Bull. Var. Stars, 1611, 2016
Mürset, U. Nussbaumer, H., Schmid, H. M., & Vogel, M. 1991, A & A, 248, 458
Nussbaumer, H. 1982, in IAU Colloq. 70, in The Nature of Symbiotic Stars, ed. M. Friedjung & R. Viotti (Dordrecht: Reidel), 85
Nussbaumer, H., Schild, H., Schmid, H. M., & Vogel, M. 1988, A&A, 198, 179
Oliverson, N. A., & Anderson, C. M. 1982, in IAU Colloq. 70, The Nature of Symbiotic Stars, ed. M. Friedjung & R. Viotti (Dordrecht: Reidel), 177
Osterbrock, D. E. 1989, Astrophysics of Gaseous Nebulae and Active Galactic Nuclei (Mill Valley, CA: Univ. Science Books)
Pottasch, S. R. 1989, Planetary Nebulae (Dordrecht: Reidel), 106
Robinson, L. 1969, Perem. Zvezdy, 16, 507
Roman, N. G. 1953, ApJ, 117, 467
Savage, B. D., & Mathis, J. S. 1979, ARA&A, 17, 73
Seaton, M. J. 1960, Rep. Progr. Phys., 23, 313
——— 1978, MNRAS, 185, 5P
——— 1979, MNRAS, 187, 73P
Slovak, M. H., Anderson, C. M. Cassinelli, J. P., & Lambert, D. L. 1987, Ap&SS, 131, 765
Viotti, R. 1993, in Cataclysmic Variables, ed. M. Hack (NASA SP), in press
Viotti, R., Altamore, A., Baratta, G. B., Cassatella, A., & Friedjung, M. 1984, ApJ, 283, 226
Viotti, R., Altamore, A., Baratta, G. B., Cassatella, A., Friedjung, M., Giangrande, A., Ponz, D., & Ricciardi, O. 1982, in Advances in Ultraviolet Astronomy: Four Years of IUE Research (NASA CP 2238), 446
Viotti, R., Ricciardi, O., Ponz, D., Giangrande, A., Friedjung, M., Cassatella, A., Baratta, G. B., & Altamore, A. 1983, A&A, 119, 285
Wilson, R. E. 1943, PASP, 55, 282